Biosensors and Bioelectronics 34 (2012) 267–272

Contents lists available at SciVerse ScienceDirect

Biosensors and Bioelectronics

journal homepage: www.elsevier.com/locate/bios

CMOS-compatible, label-free silicon-nanowire biosensors to detect cardiac troponin I for acute myocardial infarction diagnosis

Tao Kong[1], Ruigong Su[1], Beibei Zhang, Qi Zhang, Guosheng Cheng*

Suzhou Institute of Nano-Tech and Nano-Bionics, Chinese Academy of Sciences, 398 Ruoshui Road, Suzhou Industrial Park, Jiangsu 215123, China

ARTICLE INFO

Article history:
Received 4 December 2011
Received in revised form 7 February 2012
Accepted 10 February 2012
Available online 19 February 2012

Keywords:
Silicon nanowire
Field-effect transistor
Biosensor
Cardiac troponin I
Acute myocardial infarction

ABSTRACT

A label-free biosensor for electrical detection of cardiac troponin I (cTnI), a highly sensitive and selective biomarker of acute myocardial infarction (AMI), is demonstrated using silicon nanowire (SiNW) based field-effect transistors (FETs). The FET devices were fabricated by a complementary metal oxide semiconductor (CMOS) compatible top-down approach to define the SiNW followed by tetramethylammonium hydroxide (TMAH) wet etching. Electrical characterizations of the SiNW FET revealed an ambipolar conduction characteristic with an on/off ratio of 10^5–10^6. CTnI monoclonal antibodies were then covalently immobilized on the SiNW surfaces. By integrating with a homemade biosensor measurement system, the biosensor exhibited rapid and sensitive response to cTnI proteins. The current response showed a nature of logarithm relationship against the cTnI concentration from 46 ng/mL down to 0.092 ng/mL. Moreover, an anti-interference capability of the fabricated biosensor was also assessed. By utilizing the top-down fabrication method, this work provides an efficient way for the cTnI proteins detection with an enormous potential of mass-production, which definitely facilitate the practical applications.

1. Introduction

Cardiovascular diseases are the leading cause of death globally according to the World Health Organization statistics (WHO website). Among the cardiovascular diseases, acute myocardial infarction (AMI) is one of the most serious diseases that extremely affect people's health. In the past decades, several biomarkers, including creatine kinase (CK-MB), myoglobin (MYO), cardiac troponin I (cTnI) and cardiac troponin T (cTnT) have been applied for the determination of AMI (Stillman et al., 2011). Recent researches and clinical diagnosis have suggested that cTnI is a highly specific and sensitive biomarker of AMI and consequently cTnI is gradually recognized as "gold standard" for AMI diagnosis (Shen et al., 2011). Thus, fast and accurate determination of cTnI concentrations is greatly appreciated.

Generally, the cTnI levels in normal serum are below 0.6 ng/mL (approx. 24.9 pmol/L) (Boriani et al., 2000). Upon AMI, the cTnI concentration in serum dramatically increases within 3–12 h and remains raised for 5–9 days. When it reaches to 0.7–1.4 ng/mL, minor myocardial injury can be concluded, while evident myocardial necrotic damage should be considered when cTnI concentration elevates over 1.5 ng/mL (Apple et al., 1999; Boriani et al., 2000). Currently, enzyme-linked immunosorbent assay (ELISA) is frequently used in clinical diagnosis for cTnI. Though achieved a satisfied sensitivity down to 6–40 pg/mL (Tate, 2008), ELISA is still suffering from the time-consuming and laborious work. To overcome the limitation of ELISA, many methods have been developed for the enhanced detection of cTnI including electrochemiluminescence (Shen et al., 2011), fluorescence (Nandhikonda and Heagy, 2011), colorimetric method (Wu et al., 2010) and cationic isotachophoresis (Bottenus et al., 2011) etc. However, most of these methods are based on labeling technology which eventually increases the detection time and complexity of the sensor fabrication.

Nowadays, one-dimensional nanomaterials and their relevant nanodevices, especially the nanowire based field-effect transistors (FET) have been widely employed in biosensor designs. Nanowire based FET is believed to be one of the most promising devices, because of the prospect for sensitive, label-free, real time and multifunctional biosensing. Due to the chemical gating effect (Li et al., 2003), charged biomacromolecules in buffer bind with their counterparts (for example, antigen–antibody complex) initially immobilized on the nanowire surfaces to induce the change of carrier concentrations, which eventually regulates the electrical transport of FET. Taking cTnI for example, the isoelectric point (p*I*) of cTnI was experimentally measured to be around 5.2 (Peronnet et al., 2007), which makes it negatively charged in near neutral buffer systems. When binding on the nanowire surfaces, cTnI induce depletion of electrons or accumulation of holes for different types of nanowires. Since the pioneer work contributed by Lieber et al. (Cui et al., 2001), various kinds of semiconductors,

* Corresponding author. Tel.: +86 512 62872557.
E-mail address: gscheng2006@sinano.ac.cn (G. Cheng).
[1] Co-first author, equal contribution.

0956-5663/$ – see front matter © 2012 Elsevier B.V. All rights reserved.
doi:10.1016/j.bios.2012.02.019

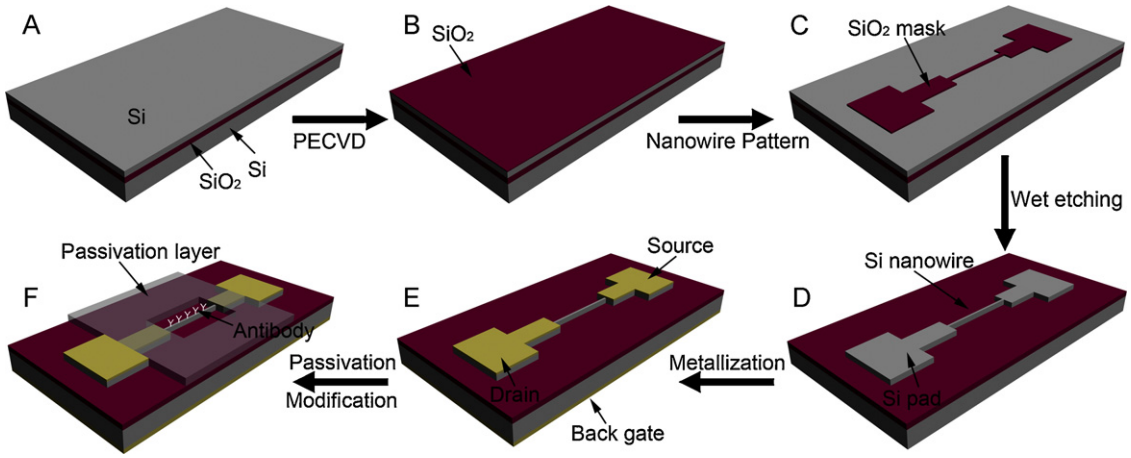

Fig. 1. Key workflow steps used for the fabrication of SiNW based FET devices. (A) Thermal oxidation to thin the device layer of SOI wafer down to ~50 nm. (B) Thin film of SiO_2 deposited by PECVD. (C) Define SiO_2 pattern by lithography. (D) Crystallographic wet etching using TMAH solution to obtain SiNWs. (E) Deposition of metal contact for Source, Drain and Back gate electrodes, followed by rapid thermal annealing to acquire ohmic contact. (F) Fabrication of SiO_2/SiN_x passivation layer by PECVD, lithography and RIE processes, followed by covalent modification of cTnI antibodies.

for example SiNWs (Ahn et al., 2010; Stern et al., 2010), SnO_2 nanowires (Cheng et al., 2011) and In_2O_3 nanowires (Ishikawa et al., 2009a,b) have been integrated in the FET type biosensors. Among these, SiNW is one of the most investigated materials due to the chemical inert property in biological solutions, ease of surface modifications and device fabrication methods (including top-down or bottom-up methods). Moreover, the fabricated biosensors based on SiNW were proven to possess the potential on numerous biosensing applications, such as DNA hybridizations (Gao et al., 2011), protein–protein interactions (Lin et al., 2010) and virus (Zhang et al., 2010) detections as well. However, less efforts have been fulfilled for the exploration of AMI biomarkers biosensing (Chua et al., 2009).

Herein, SiNW based FETs were fabricated by a top-down approach and used as a label-free cTnI protein biosensor. The SiNWs were acquired by TMAH wet etching and then functionalized with cTnI monoclonal antibodies. The fabrication processes were highly CMOS-compatible with mass-production ability. The electrical transport, biosensor performance and anti-interference abilities of the biosensor have been quantified.

2. Materials and methods

2.1. Materials

SOI wafers (6 in., p-type (1 0 0), ρ: 10–20 Ω cm) were purchased from Shanghai Simgui Technology Co., Ltd. Aldehyde, (3-aminopropyl)triethoxysilane (APTES), glutaraldehyde, ethanolamine, phosphate buffered saline (PBS, pH 7.4) and bovine serum albumin (BSA) were obtained from Sigma–Aldrich and used as received without further purification. 25% (w/w) tetramethylammonium hydroxide (TMAH, 99.9999%) solution was purchased from Alfa-Aesar. CTnI protein and its monoclonal antibody were provided by Jiangsu Province hospital (China). All solutions were prepared with deionized water (DI, $R \geq 18.2$ MΩ cm) generated from a Millipore system.

2.2. Fabrication of Si Nanowire based field-effect transistors

The general route for the fabrication of SiNW based FET is outlined in Fig. 1. Due to the sensitivity of SiNW biosensor is significantly affected by the size of SiNWs, we first thinned the thickness of top layer of SOI wafer down to ~50 nm using thermal oxidation process. 20 nm SiO_2 thin film was then deposited on the SOI wafer using plasma enhanced chemical vapor deposition (PECVD) for the fabrication of SiO_2 mask. By employing Nikon stepper lithography equipment (Nikon NSR 1755i B), SiO_2 pattern can be obtained as shown in Fig. 1C. In this process, the critical dimension of the SiO_2 pattern was designed to be 700 nm. After that, the wafer was transferred into a culture dish containing 100 mL 25% TMAH solution for wet etching. The wet etching rate for Si is dependent upon the temperature and time. In this work, for the fabrication of <100 nm SiNWs, we performed the wet etching at 70 °C for around 23.5 min. To define source, drain and back gate contacts, Ni/Au (20 nm/100 nm) bilayer was then deposited on the wafer, in which Ni acted as an adhesion layer while Au provided electrical connection between nanodevices and measurement equipment. The wafer was then annealed at 400 °C to obtain ohmic contact using rapid thermal annealing. During the measurements in aqueous solutions, the chips usually suffer from the water molecules and ions resulting in malfunction. Besides, currents flow between metal contacts through solution can also cause interferences for the biosensor. In order to avoid such limits, passivation layer composed of SiO_2/SiN_x (100 nm/100 nm) bilayer structure was introduced using PECVD followed by lithography (to open the SiNW detection window), reaction ion etching (RIE, to remove SiN_x layer of SiNW region) and buffered oxide etching (5:1 BOE, to remove SiO_2 layer) as shown in Fig. 1F.

2.3. Modification of the cTnI antibody on Si nanowires

SiNWs can be covalently modified with cTnI monoclonal antibodies through the natural oxidation layer (~2 nm) of SiNWs. In this work, prior to immobilize the cTnI antibody on the SiNWs, aldehyde was first utilized to modify the SiN_x layer to avoid protein adsorption on the passivation layer. SOI wafer with fabricated SiNW FETs was dipped into 20% aldehyde aqueous solution for 30 min to modify the amino groups on the SiN_x surface. After intense DI rinse, the wafer was loaded into 1% APTES ethanol solution for 45 min followed by 120 °C treatment for 1 h to remove loosely bonded APTES molecules. APTES treatment can introduce $-NH_2$ groups onto the SiNW surfaces. Then, the wafer was dipped into 2.5% glutaraldehyde aqueous solution for 1 h. After thorough washing with DI, the wafer was immersed into a solution containing 1 mg/mL cTnI antibody in PBS buffer (pH 7.4) at 4 °C for overnight. Finally, the residual aldehyde groups and unspecific binding sites on the SiNWs were blocked by 50 mM ethanolamine in PBS buffer for 1 h and 1 mg/mL BSA for 4 h at room temperature, respectively. The wafer was stored in dry condition at 4 °C when not in use.

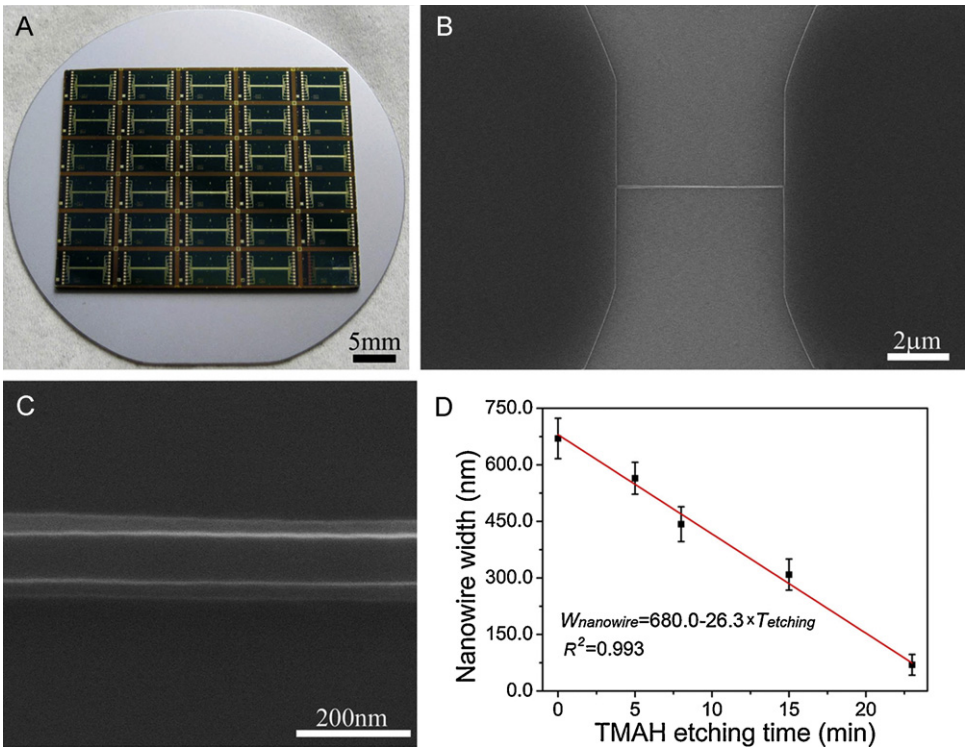

Fig. 2. (A) Optical image of the fabricated SiNW FET arrays. (B) SEM image of a typical SiNW region. (C) SEM image of a single SiNW. (D) The SiNW width varied with the TMAH etching time.

2.4. Device characterizations and biosensing setup

Scanning electron microscopy (SEM, Quanta 400 FEG, FEI Company, USA) was employed to characterize the morphology of the fabricated devices. The devices used for electrical measurements and biosensing experiments were similar in nanowire height and width. For the transport properties of the SiNW based FETs, measurements were performed using an Agilent B1500A semiconductor device analyzer (Agilent Technologies Inc., USA). The biosensor measurements were accomplished using a homemade biosensor measurement system, in which a peristaltic pump was integrated to transport the solution from sample vessels to the liquid cells with a speed of 20 μL/min. The volume of liquid cell was 50 μL and kept the same during measurements. The measurements were performed at room temperature (25 ± 2 °C).

3. Results and discussion

3.1. Morphology of the fabricated Si nanowire based field-effect transistors

Nanodevices fabricated with top-down methods result in a uniform dimension and morphologies with mass-production feature. Furthermore, the CMOS-compatible fabrication processes allow the nanodevices to be easily integrated with the semiconductor industry, which facilitates the commercialization of nanodevices in the practical applications. The SOI wafers were first thinned down to 53.0 ± 0.11 nm measured by an ellipsometer (M2000D, J.A. Woollam Co., USA). Dry etching including RIE, IBE (ion beam etching) etc. and wet etching are common methods used in the fabrication of SiNWs with a top-down approach. However, the dry etching usually causes rough surfaces and the charged ions accumulates on the SiNW surfaces which may result in degraded device performances. In contrast, the wet etching using TMAH acquires smooth surfaces. Besides, due to the TMAH etching is of an anisotropic etching, the etching rate of (1 0 0) planes is much faster than that of (1 1 1) planes, which commonly causes a trapezoidal cross-section with dominant (1 1 1) planes for SiNWs. This feature is benefit for the biomolecules modifications (Bunimovich et al., 2004). Herein, we employed TMAH as etchant for the fabrication of SiNWs. Fig. 2A shows an optical image of SiNW FET arrays. The dimension of a single cell is 7.5 mm × 5 mm. Fig. 2B displays SEM image of a representative nanowire region with a length of 5 μm. The detailed SiNW image is demonstrated in Fig. 2C. It can be seen that the SiNW is of trapezoid shape with (1 0 0) planes for top layer and (1 1 1) planes for lateral surfaces. The average width of the top layer in Fig. 2C is measured to be around 80 nm. By using TMAH wet etching, the width of SiNWs can be readily adjusted by the etching time. After Nikon stepper lithography process, the critical dimension of SiO_2 pattern was measured to be around 670 nm. We performed a series of TMAH etching experiments and concluded that the SiNW width versus the etching time followed the equation: $W_{nanowire}(\text{nm}) = 680.0 - 26.3 \times T_{etching}(\text{min})$, where $W_{nanowire}$ for SiNW width and $T_{etching}$ for TMAH etching time.

3.2. Electrical characterizations of the Si nanowire based field-effect transistors

The electrical characterizations including output and transport behaviors of the SiNW based FET are presented in Fig. 3. As depicted in the transport behavior (inset of Fig. 3), strong gate dependence was observed with an on/off ratio of 10^5–10^6. The FET also exhibited an ambipolar conduction characteristic which is consistent with previous observations (Elfstrom et al., 2008; Elfstrom and Linnros, 2008). The mechanism for positive gate voltage conduction is originated from the electrons in inversion layer while the negative gate voltage indicates an accumulation mode with holes as conduction species (Elfstrom et al., 2008; Elfstrom and Linnros, 2008). Additionally, small hysteresis phenomenon between forward (F) and

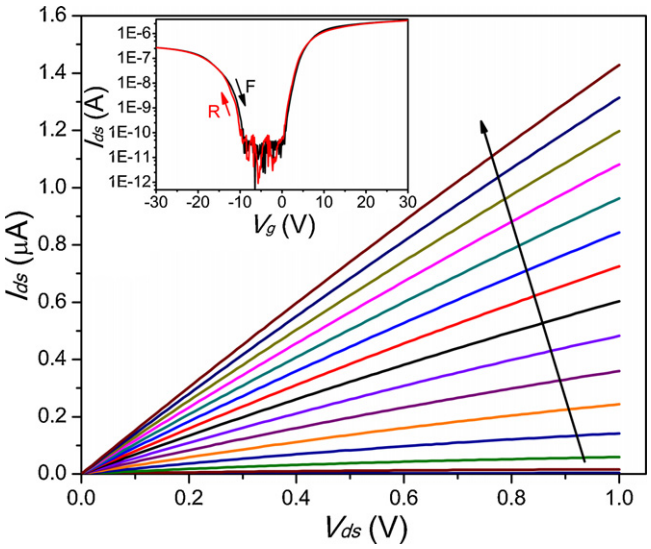

Fig. 3. Electrical output characterization of SiNW based FET. The Gate voltage varied from −10 V to 10 V in +1 V steps as the arrow indicated. The inset is the transport behavior for a constant V_{ds} = 1 V for forward (F) and reverse (R) sweep of a SiNW based FET.

reverse (R) sweeps confirms the minimal defects induced charge trapping (Stern et al., 2007).

3.3. Response behaviors of the cardiac troponin I biosensor

After the electrical characterizations of the fabricated SiNW FETs, the devices were then assembled in the homemade biosensor measurement system. The volume of liquid cell kept the same through the whole measurements to avoid the interference of solution volume change to the biosensing signals. Linear regime, near threshold regime and subthreshold regime of a nanowire FET working regime can be chosen in the biosensing applications; however, the subthreshold regime has the optimal sensitivity for detection of biomacromolecules using nanowire based FET biosensors, due to the reduced screening of carriers in nanowires (Gao et al., 2010). In this work, we applied V_g = 2.5 V located in the subthreshold regime (V_T = 4.4 V) and V_{ds} = 0.2 V for the following biosensing measurements.

Fig. 4 illustrates the biosensing results for the detection of cTnI protein in 0.1× PBS solutions. As seen from Fig. 4A, the biosensor exhibited a constant and stable response for blank PBS solution over 2000 s, further confirmed an excellent stability of the biosensor devices and the measurement system. When certain concentrations of cTnI solutions were loaded into the liquid cell, an apparent current change was observed accordingly as shown in Fig. 4B and C. However, there existed around 30 s delay between addition of cTnI solutions and the corresponding response, which might result from the diffusion of cTnI proteins to the SiNW surfaces. After binding events between cTnI proteins and their antibodies occurred on the SiNW surfaces, the biosensor reached a steady-state current in 30 s and maintained for over 200 s. By calculating the biosensor response to various concentrations of cTnI solutions, a calibration curve was plotted as shown in Fig. 4D. The limit of detection of the SiNW based FET for the detection of cTnI was 0.092 ng/mL (signal/noise ratio of 3). Logarithm relationship was observed between the current change ratio and cTnI concentration (C_{cTnI}) from 0.092 ng/mL to 46 ng/mL. The calibration curve can be fitted as $\Delta I/I_0 = 0.180 + 0.065 \times \ln C_{cTnI}$, where I_0 stood for the background I_{ds}, ΔI for the I_{ds} change between background and

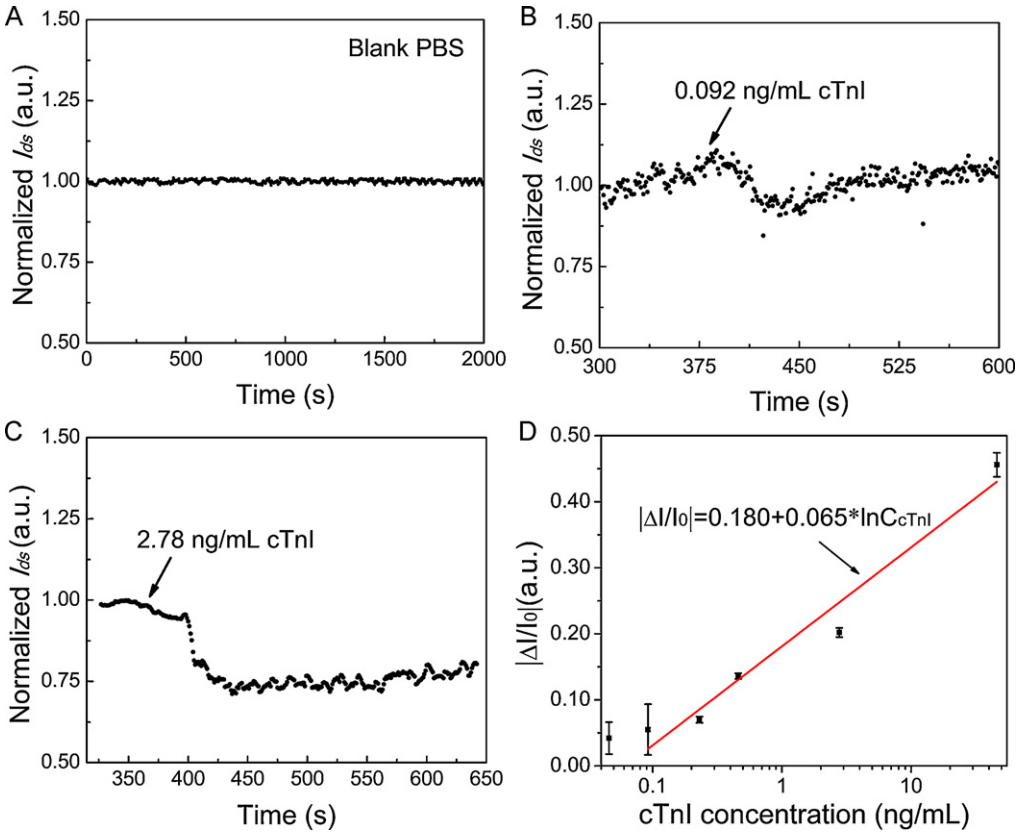

Fig. 4. Real-time detection of various concentrations of cTnI protein with SiNW based FET biosensor. Normalized I_{ds} in blank 0.1× pH 7.4 PBS (A) and upon addition of 0.092 ng/mL (B) and 2.78 ng/mL (C) cTnI protein solution. Normalized I_{ds} change versus the logarithm of cTnI protein concentrations (D).

Table 1
Comparison of the linear dynamic range and limit of detection of cTnI biosensors based on various methods.

Methods	Materials	Linear range (ng/mL)	Limit of detection (ng/mL)	Ref.
Electrochemical immunoassay	MCM-41 mesoporous material	0.8–5.0	0.5	Guo et al. (2005a)
Electrochemical immunoassay	Silver enhancement on gold nanoparticle	1–20	0.8	Guo et al. (2005b)
Optomagnetic method	Superparamagnetic particles	0.03–6.5	0.03	Dittmer et al. (2010)
Guided-mode resonance (GMR) biosensor	GMR filter chips	0.05–10	0.05	Kim et al. (2010)
Electrochemiluminescence immunosensor	Functionalized gold nanoparticles	0.0025–10	0.002	Shen et al. (2011)
FET nanodevice	Si nanowire	0.092–46	0.092	This work

upon addition of cTnI. The biosensor response showed logarithmic dependence on the target protein concentrations, which was presented in the nanowire FET-type biosensors (Gao et al., 2011). This observation was also in consistent with the theoretical simulations, in which the inherent nonlinear screening caused by the electrolyte of the measurement system (Nair and Alam, 2008). Table 1 summarizes cTnI biosensors based on various methods and materials. From Table 1, the proposed SiNW FET biosensor possesses quite wide linear dynamic range and relative low detection limit for the detection of cTnI with respect to previous reports.

In the biosensor design and integration processes, the specific detection ability needs careful considerations. Many methods have been adopted for minimization of non-specific protein bindings, in which the BSA blocking is regarded as an efficient approach (Hideshima et al., 2011). After the cTnI antibodies covalently modified on the SiNW surfaces, BSA was applied as a blocking agent. Fetal bovine serum (FBS) was chosen as an interference specie, since FBS was widely used in cell culture, cell engineering and other biological areas, containing various proteins with a total concentration of approximately 42 mg/mL (Alley et al., 1988). As shown in Fig. 5, PBS buffer containing 10% FBS (the diluted total protein concentration of about 4.2 mg/mL) was first measured as background. When 0.23 ng/mL cTnI solution (0.1× PBS containing 10% FBS as solvent) was added into the buffer, ~6.4% current change was observed, in accordance with the calibration curve in Fig. 4D (~7.0% for 0.23 ng/mL cTnI in pure PBS buffer). The sensing ability of a nanowire FET-type biosensor is greatly influenced by the Debye screening length. For 0.1× PBS, the Debye length is typically ~2.3 nm (Chua et al., 2009) and will be decreased after adding of FBS with relative high salt concentrations. However, according to the acquired results, the Debye length was still sufficiently long enough for detection of cTnI proteins under the experimental conditions. Additionally, considering the protein concentration of diluted FBS was greatly higher than that of cTnI, we then concluded that the fabricated biosensor can also eliminate most of the non-specific protein bindings.

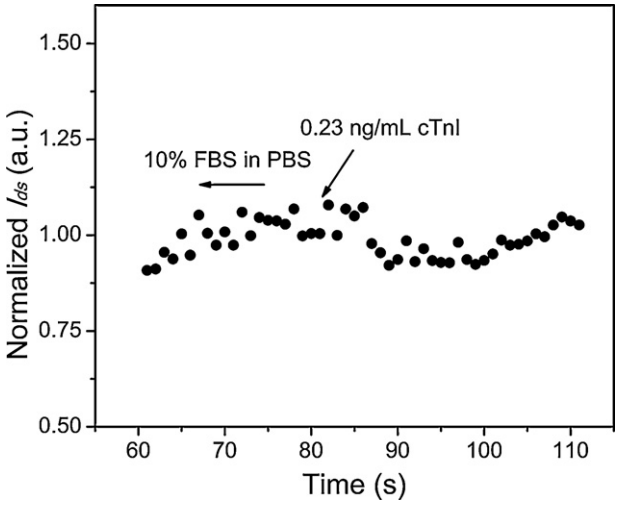

Fig. 5. Typical anti-interference ability of the biosensor. 0.1× PBS containing 10% FBS was chosen as model interference and used as background. 0.23 ng/mL cTnI solution was added into the PBS buffer inducing ~6.4% current change.

4. Conclusions

In summary, we demonstrated a SiNW based FET device for sensitive and selective analysis of AMI biomarker, cTnI. The FET device was fabricated with top-down method which was preferentially CMOS-compatible with mass-production ability. An ambipolar conductance behavior was observed for the fabricated FET devices. After modifications of cTnI antibodies onto the SiNW surfaces, the biosensor showed a sensitive and rapid response for the cTnI protein with a logarithm relationship between the current response and the cTnI concentration. Additionally, the biosensor possessed an acceptable anti-interference ability. The results presented in this work suggest that the SiNW based FET biosensor have potential applications in the clinical diagnosis of AMI.

Acknowledgements

This work was partially funded by the National Basic Research Program of China (973 Program) under award numbers of 2011CB965004, 2009CB930802, National Natural Science Foundation of China (NSFC) (Grant numbers: 10834004 & 11104317) and "Hundred Talents Program" of Chinese Academy of Sciences. We are grateful for the professional services offered by the Platforms of Characterization & Test and Nanofabrication Facility at Suzhou Institute of Nano-Tech and Nano-Bionics, Chinese Academy of Sciences.

References

Ahn, J.H., Choi, S.J., Han, J.W., Park, T.J., Lee, S.Y., Choi, Y.K., 2010. Nano Lett. 10, 2934–2938.
Alley, M.C., Scudiero, D.A., Monks, A., Hursey, M.L., Czerwinski, M.J., Fine, D.L., Abbott, B.J., Mayo, J.G., Shoemaker, R.H., Boyd, M.R., 1988. Cancer Res. 48, 589–601.
Apple, F.S., Maturen, A.J., Mullins, R.E., Painter, P.C., Pessin-Minsley, M.S., Webster, R.A., Flores, J.S., DeCresce, R., Fink, D.J., Buckley, P.M., Marsh, J., Ricchiuti, V., Christenson, R.H., 1999. Clin. Chem. 45, 206–212.
Boriani, G., Biffi, M., Cervi, V., Bronzetti, G., Magagnoli, G., Zannoli, R., Branzi, A., 2000. Chest 118, 342–347.
Bottenus, D., Hossan, M.R., Ouyang, Y., Dong, W.J., Dutta, P., Ivory, C.F., 2011. Lab Chip 11, 3793–3801.
Bunimovich, Y.L., Ge, G.L., Beverly, K.C., Ries, R.S., Hood, L., Heath, J.R., 2004. Langmuir 20, 10630–10638.
Cheng, Y., Chen, K.S., Meyer, N.L., Yuan, J., Hirst, L.S., Chase, P.B., Xiong, P., 2011. Biosens. Bioelectron. 26, 4538–4544.
Chua, J.H., Chee, R.E., Agarwal, A., Wong, S.M., Zhang, G.J., 2009. Anal. Chem. 81, 6266–6271.
Cui, Y., Wei, Q.Q., Park, H.K., Lieber, C.M., 2001. Science 293, 1289–1292.
Dittmer, W.U., Evers, T.H., Hardeman, W.M., Huijnen, W., Kamps, R., de Kievit, P., Neijzen, J.H.M., Nieuwenhuis, J.H., Sijbers, M.J.J., Dekkers, D.W.C., Hefti, M.H., Martens, M.F.W.C., 2010. Clin. Chim. Acta 411, 868–873.
Elfstrom, N., Karlstrom, A.E., Linnrost, J., 2008. Nano Lett. 8, 945–949.
Elfstrom, N., Linnros, J., 2008. Nanotechnology 19, 235201.
Gao, A.R., Lu, N., Dai, P.F., Li, T., Pei, H., Gao, X.L., Gong, Y.B., Wang, Y.L., Fan, C.H., 2011. Nano Lett. 11, 3974–3978.
Gao, X.P.A., Zheng, G.F., Lieber, C.M., 2010. Nano Lett. 10, 547–552.
Guo, H.S., He, N.Y., Ge, S.X., Yang, D., Zhang, J.N., 2005a. Talanta 68, 61–66.
Guo, H.S., Zhang, J.N., Xiao, P.F., Nie, L.B., Yang, D., He, N.Y., 2005b. J. Nanosci. Nanotechnol. 5, 1240–1244.

Hideshima, S., Sato, R., Inoue, S., Kuroiwa, S., Osaka, T., 2011. Sens. Actuators B: Chem., doi:10.1016/j.snb.2011.10.001.
Ishikawa, F.N., Chang, H.K., Curreli, M., Liao, H.I., Olson, C.A., Chen, P.C., Zhang, R., Roberts, R.W., Sun, R., Cote, R.J., Thompson, M.E., Zhou, C.W., 2009a. ACS Nano 3, 1219–1224.
Ishikawa, F.N., Curreli, M., Chang, H.K., Chen, P.C., Zhang, R., Cote, R.J., Thompson, M.E., Zhou, C.W., 2009b. ACS Nano 3, 3969–3976.
Kim, W.J., Kim, B.K., Kim, A., Huh, C., Ah, C.S., Kim, K.H., Hong, J., Park, S.H., Song, S., Song, J., Sung, G.Y., 2010. Anal. Chem. 82, 9686–9693.
Li, C., Lei, B., Zhang, D.H., Liu, X.L., Han, S., Tang, T., Rouhanizadeh, M., Hsiai, T., Zhou, C.W., 2003. Appl. Phys. Lett. 83, 4014–4016.
Lin, T.W., Hsieh, P.J., Lin, C.L., Fang, Y.Y., Yang, J.X., Tsai, C.C., Chiang, P.L., Pan, C.Y., Chen, Y.T., 2010. Proc. Natl. Acad. Sci. 107, 1047–1052.
Nair, P.R., Alam, M.A., 2008. Nano Lett. 8, 1281–1285.
Nandhikonda, P., Heagy, M.D., 2011. J. Am. Chem. Soc. 133, 14972–14974.
Peronnet, E., Becquart, L., Martinez, J., Charrier, J.P., Jolivet-Reynaud, C., 2007. Clin. Chim. Acta 377, 243–247.
Shen, W., Tian, D.Y., Cui, H., Yang, D., Bian, Z.P., 2011. Biosens. Bioelectron. 27, 18–24.
Stern, E., Klemic, J.F., Routenberg, D.A., Wyrembak, P.N., Turner-Evans, D.B., Hamilton, A.D., LaVan, D.A., Fahmy, T.M., Reed, M.A., 2007. Nature 445, 519–522.
Stern, E., Vacic, A., Rajan, N.K., Criscione, J.M., Park, J., Ilic, B.R., Mooney, D.J., Reed, M.A., Fahmy, T.M., 2010. Nat. Nanotechnol. 5, 138–142.
Stillman, A.E., Oudkerk, M., Bluemke, D., Bremerich, J., Esteves, F.P., Garcia, E.V., Gutberlet, M., Hundley, W.G., Jerosch-Herold, M., Kuijpers, D., Kwong, R.K., Nagel, E., Lerakis, S., Oshinski, J., Paul, J.F., Underwood, R., Wintersperger, B.J., Rees, M.R., 2011. Int. J. Cardiovasc. Imaging 27, 7–24.
Tate, J.R., 2008. Clin. Chem. Lab. Med. 46, 1489–1500.
WHO website, 2012. http://www.who.int/mediacentre/factsheets/fs317/en/index.html (accessed 07.02.12).
Wu, W.Y., Bian, Z.P., Wang, W., Wang, W., Zhu, J.J., 2010. Sens. Actuators B: Chem. 147, 298–303.
Zhang, G.J., Zhang, L., Huang, M.J., Luo, Z.H.H., Tay, G.K.I., Lim, E.J.A., Kang, T.G., Chen, Y., 2010. Sens. Actuators B: Chem. 146, 138–144.